Available online at www.sciencedirect.com
ScienceDirect
Nuclear Physics B Proceedings Supplement 00 (2012) 1–12
Nuclear Physics B Proceedings Supplement

Recent QCD results from the Tevatron

Markus Wobisch

Louisiana Tech University, Ruston, LA, USA

Abstract

Recent QCD related results from the CDF and the DØ experiments are presented based on proton anti-proton collision data at $\sqrt{s} = 1.96\,\text{TeV}$, taken in Run II of the Fermilab Tevatron Collider. Measured observables include inclusive photon and diphoton production, vector boson plus jets production, event shape variables, and inclusive multijet production. The measurement results are compared to QCD theory calculations in different approximations. A determination of the strong coupling constant from jet data is presented.

Keywords: QCD test, jet production, photon production, vector boson plus jet production, event shapes, strong coupling constant

1. Introduction

This presentation was given two days before the Fermilab Tevatron Collider had stopped its operations. During the previous ten years, in Run II, the Tevatron had delivered an integrated luminosity of $12\,\text{fb}^{-1}$ of proton-antiproton collisions at a center of mass energy of 1.96 TeV to the CDF and DØ experiments, with peak luminosities of up to $4.3 \cdot 10^{32}\,\text{cm}^{-2}\text{s}^{-1}$.

This article presents an overview of recent QCD results from the CDF and the DØ experiments, based on data sets with integrated luminosities of $0.7 - 8.2\,\text{fb}^{-1}$. Presented are measurements of inclusive isolated photon and diphoton production, vector boson plus jet production for different jet multiplicities, and event shape variables. Also presented are measurement results of multijet production together with phenomenological analyses to constrain the parton distribution functions (PDFs) of the proton and to determine the strong coupling constant, α_s. In all cases, the data are corrected for instrumental effects and are presented at the "particle level," which includes all stable particles as defined in Ref. [1]. The results are used to test either particle-level predictions by Monte Carlo events generators, or perturbative QCD (pQCD) calculations in fixed order in α_s which are corrected for non-perturbative effects.

2. Photon Production

Photon cross sections in hadron collisions receive contributions from "prompt" photons which directly emerge from the hard subprocess, and from photons which are produced in the fragmentation of energetic π^0 and η mesons. The latter are usually accompanied by hadrons, and their contribution can be significantly reduced by requiring the photon to be isolated from other particles in the event. Isolated photon cross sections are therefore dominated by prompt photons. At lowest order, prompt photons are produced via quark-gluon Compton scattering or quark-antiquark annihilation, and are therefore directly sensitive to the dynamics of the hard subprocess and to α_s and the PDFs of the hadrons. Furthermore, diphoton final states are also signatures for various new physics processes, such as extra spatial dimensions and for heavy new particles, such as the Higgs boson, decaying into photons.

2.1. Inclusive Isolated Photon Production

Photon production has been considered an ideal source of direct information on the gluon density in the proton [2, 3]. However, it was observed [4] that not all experimental data are consistently described by pQCD calculations in fixed order of α_s. On the one hand, it was

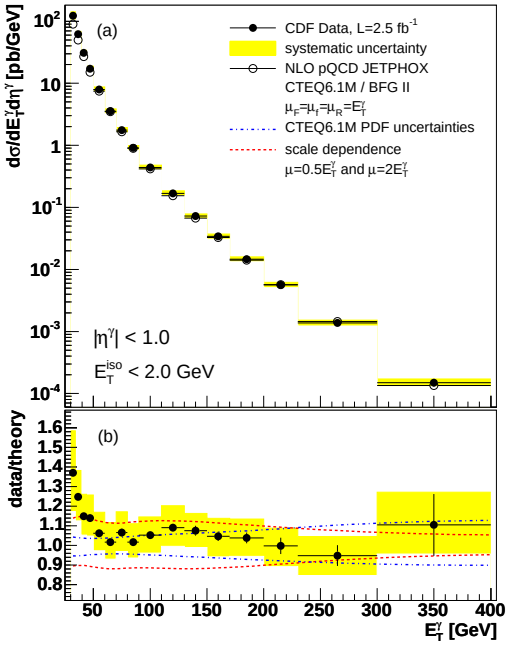

Figure 1: CDF measurement of the inclusive isolated photon cross section, measured differentially in photon E_T.

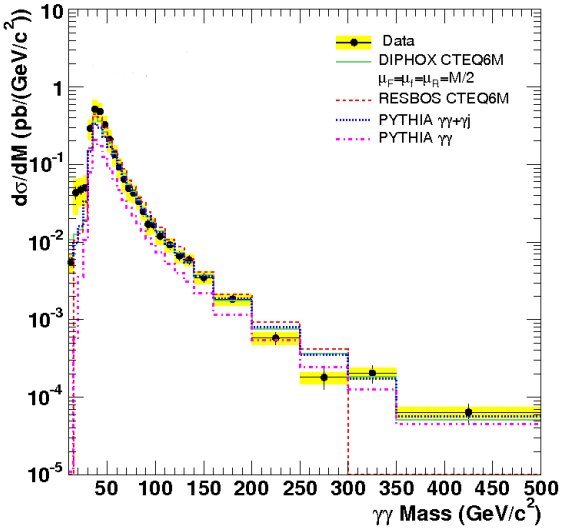

Figure 2: CDF measurement of the diphoton invariant mass dependence of the diphoton cross section.

argued that the existing data may not be consistent [4]. It was also suggested that the phenomenological introduction of an intrinsic transverse momentum of the incoming partons may help improve the description of the data and reduce the inconsistencies [5]. But this ad-hoc procedure still had a significant model dependence and was not seen to be a fundamental solution. In recent global PDF fits photon data have been excluded [6, 7, 8].

In order to rescue the photon data as a source of additional information on the PDFs, it is important either to identify critical missing pieces in theory or to clearly establish inconsistencies of existing data sets. Precision measurements in new kinematic regions are vital for testing theory predictions.

Earlier in Run II, the CDF and DØ experiments had each measured the inclusive isolated photon cross section [9, 10]. The CDF results are shown in Fig. 1 as a function of the photon transverse energy. The pQCD predictions are computed in next-to-leading order (NLO) in α_s using the program JETPHOX [11, 12] with CTEQ6.1M PDFs [13], and renormalization and factorization scales set to $\mu_{R,F} = E_T^\gamma$. The E_T^γ dependence of the data/theory ratio is consistent with what was observed by DØ, and by previous isolated photon measurements in collider and fixed target experiments at lower energies.

To investigate the potential sources of disagreement in more detail, the DØ collaboration has subsequently measured this cross section more differentially [14]. For this purpose, also the jet (produced in association with the photon) was tagged, and the photon plus jet cross section was measured in four regions of the photon and jet rapidities: For central jets ($|y_{\rm jet}| < 0.8$) and for forward jets ($1.5 < |y_{\rm jet}| < 2.5$), and in each case for same side photons ($y_\gamma \cdot y_{\rm jet} > 0$) and for opposite side photons ($y_\gamma \cdot y_{\rm jet} < 0$). Again, in none of these rapidity regions could theory describe the E_T^γ dependence observed in data.

In an additional measurement [15], the DØ collaboration has measured the photon plus jet production cross section, this time, however, for heavy flavor jets (separately for c- and b-jets, both at central rapidities). While the photon plus c-jet cross section is not described by theory, NLO pQCD theory is in good agreement with the measured photon plus b-jet cross sections. This result is consistent with a measurement of the photon plus b-jet cross section by the CDF collaboration [16].

A possible conclusion could be that the additional hard scale, provided by the heavy quark, improves the fixed-order pQCD theory calculation.

2.2. Diphoton Cross Section

The leading contributions to diphoton production are from quark-antiquark annihilation and from gluon-gluon-scattering. Although the latter process is sup-

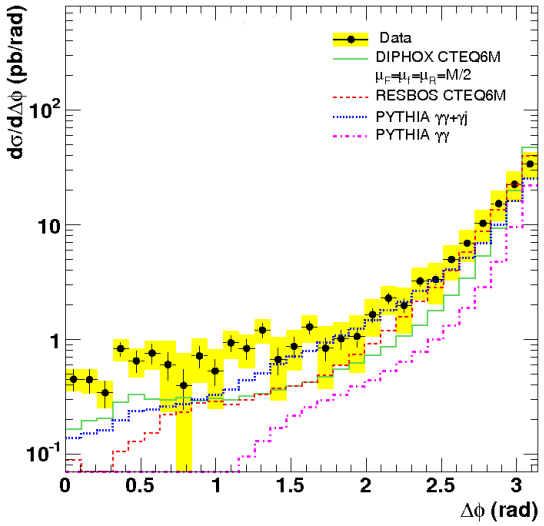

Figure 3: CDF measurement of the diphoton $\Delta\phi$ distribution of the diphoton cross section.

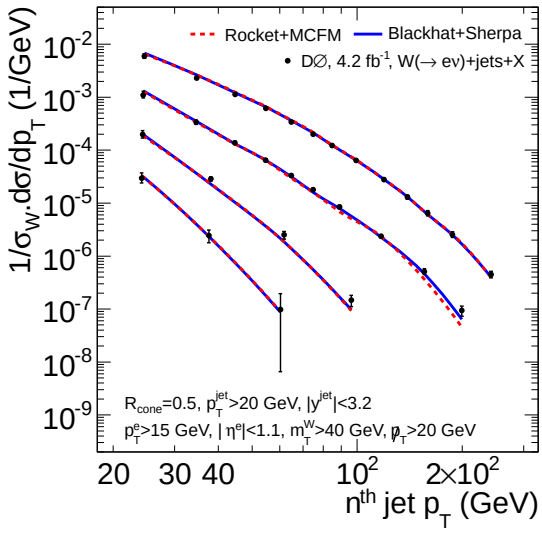

Figure 4: DØ measurement of the production cross section for $W + n$ jets, differentially in p_T of the jets. The data are compared to different pQCD calculations in NLO (for $n \leq 3$) and LO (for $n = 4$).

pressed by a factor of α_s^2 (as the photons couple to a quark box), its contribution is still significant at small diphoton masses. In this kinematic range the PDFs are probed at small momentum fractions, where the gluon density is much larger than the quark densities. In addition to the prompt contributions, the diphoton cross section also receives contributions where one or two photons are produced in fragmentation processes.

The CDF and DØ collaborations have both measured the diphoton cross section [17, 18] as a function of diphoton invariant mass, diphoton transverse momentum, and the azimuthal angle difference $\Delta\phi$ between the two photons. The results are compared to different approximations of pQCD. The program DIPHOX [11] includes NLO matrix elements for both the direct contribution and the fragmentation contribution. The contributions from fragmentation processes are especially large in the regions of small diphoton masses, large p_T, and small $\Delta\phi$. The program RESBOS [19] has implemented the fragmentation contributions only at LO, but it includes resummation of soft initial-state gluon radiation which are especially relevant at low diphoton p_T and at large $\Delta\phi$. The data are also compared to the results from PYTHIA [20] (LO matrix elements plus parton shower and fragmentation model). The diphoton invariant mass and $\Delta\phi$ distributions are shown in Figs. 2 and 3, respectively. The DIPHOX (solid line) and RESBOS (dashed line) predictions both give a reasonable overall description of the data, except in specific "critical kinematic regions" in which the unique features of the different calculations are probed. The diphoton mass distribution is described by both for masses above the peak at 30 GeV, while both underestimate the cross section at lower masses. For the diphoton p_T distribution (not shown) only RESBOS can describe the data for $p_T < 20$ GeV, the region where soft gluon resummation is most important. Discrepancies between data and theory are most prominent in the comparison of the measured and predicted distributions of $\Delta\phi$, where none of the predictions can describe the whole spectrum. However, in the region $\Delta\phi \rightarrow \pi$, where soft gluon processes are expected to become relevant, the RESBOS prediction agrees better with the data. At smallest values, $\Delta\phi < 1$, corresponding to the region of smallest diphoton masses, the DIPHOX prediction which includes the additional fragmentation contributions is closer to the data.

For a better overall description of diphoton production, it would be desirable to have a single calculation which includes all of the existing pieces, the full NLO calculations of the direct and fragmentation contributions, combined with $O(\alpha_s^3)$ $gg \rightarrow \gamma\gamma$ corrections plus resummed initial-state contributions.

3. Vector Boson plus Jet Production

Measurements of the production rates of vector bosons plus jets provide fundamental tests of pQCD in different approximations. Available predictions include

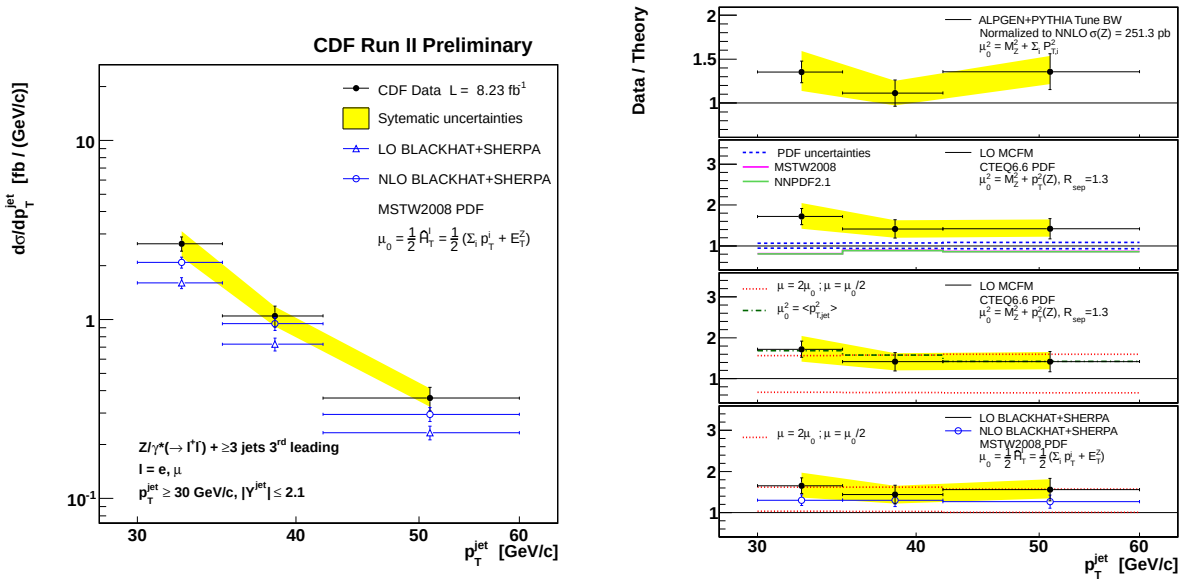

Figure 5: CDF Measurement results for the production cross section for Z/γ^* + 3 jets, differentially in p_T of the third jet (left). The data are compared to pQCD predictions in LO and NLO. Ratios of data and theory are shown on the right. The ratios to LO and NLO pQCD are in the bottom figure ("BLACKHAT+SHERPA").

calculations in fixed order in α_s, MC generators using leading order matrix elements plus parton shower, or matched tree-level matrix elements combined with parton showers. While the former are fundamental for precise quantitative tests of the theory, the latter are important tools for estimating backgrounds in many searches of new physics signals. These processes can also constitute the dominant backgrounds for single top and $t\bar{t}$ production, for searches of the Higgs boson, and for searches of new physics signatures beyond the standard model. Especially, Z boson plus b jet production is a significant background for associated Standard Model Higgs production ($ZH \to Zb\bar{b}$) and for searches of supersymmetric partners of the b quark.

The production rates of heavy vector bosons accompanied by jets have been studied in Run II in a large number of measurements. These include measurements of jet p_T spectra and angular distributions of the jet or the jet-Z/W system [21, 22, 23, 24]. Further analyses have measured the production rates of a Z/W accompanied by a heavy (c or b quark) jet [25, 26, 27, 28]. Here, two recent measurements of Z + jet and W + jet production by the CDF and the DØ collaboration, respectively, are presented. Both collaborations have measured jet p_T spectra in $Z/W + n$ jet production for $n = 1, 2, 3, 4$. These measurements constitute the first tests of NLO pQCD predictions for Z/W + 3 jet production.

3.1. W plus Jet Production

The inclusive W ($\to e\nu_e$) plus n jet production cross section is measured in the DØ experiment for $n = 1, 2, 3, 4$ using a data sample corresponding to 4.2 fb^{-1} [29]. Jets are reconstructed using the Run II midpoint cone jet algorithm with cone radius $R = 0.5$. The $W + n$ jet events are selected by requirements on the central electron ($p_T > 15$ GeV), the missing transverse energy ($\not\!\!E_T > 20$ GeV), the transverse mass of the W boson candidate ($M_T^W > 40$ GeV), and the jet transverse momenta ($p_T > 20$ GeV). In addition, the spatial distance (in η, ϕ) between the electron and the nearest jet is required to be $\Delta R > 0.5$. Acceptance corrections and background contributions from Z + jets, $t\bar{t}$, diboson, and single top production are estimated using different Monte Carlo event generators [29]. The backgrounds from multijet production are determined using a data driven method. After background subtraction, the differential distributions in jet p_T are corrected for experimental effects, and the corrected differential cross sections are normalized to the measured inclusive W boson cross section. The results are displayed in Fig. 4 as a function of p_T (separately for the first, second, third and fourth jet) and compared to pQCD predictions in NLO (for $n \leq 3$) or LO (for $n = 4$) which have been corrected for non-perturbative effects. The theory predictions have been obtained using the generators BLACKHAT+SHERPA [30] (solid line) and ROCKET + MCFM [31, 32]

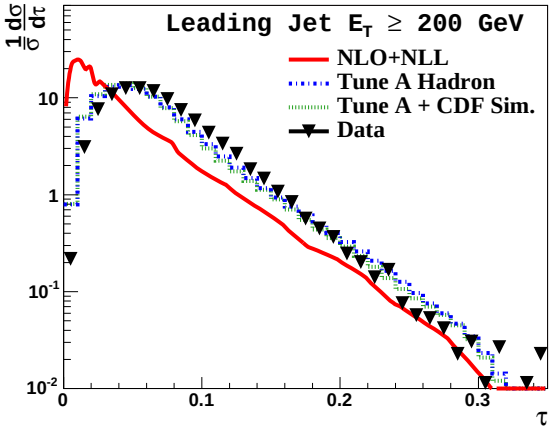

Figure 6: CDF measurement of the differential distribution of the event shape variable transverse thrust.

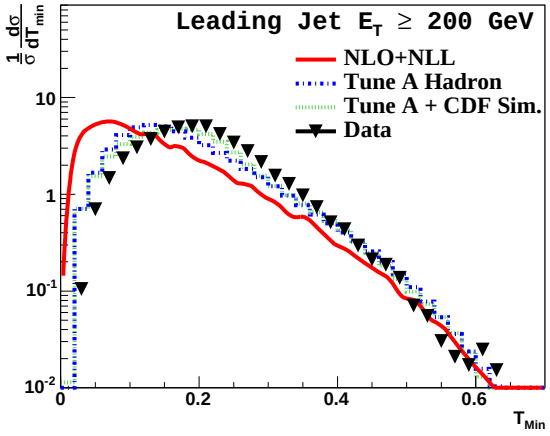

Figure 7: CDF measurement of the differential distribution of the event shape variable transverse thrust minor.

(dashed line). In general, within their uncertainties, the NLO pQCD predictions reproduce the data, except in a few regions (the low p_T region for W + 1 jet where theory is slightly higher, and the high p_T region for W + 3 jets where theory is slightly lower than the data). The LO predictions for W + 4 jets describe the data well, but they are subject to huge uncertainties from the renormalization scale dependence.

3.2. Z plus Jet Production

The CDF collaboration has presented a preliminary measurement of the Z/γ^* ($\rightarrow l^+l^-$) + n jet cross section (for n=1,2,3,4), where $l^\pm = e^\pm$ or $\mu^\pm$ [33]. A comprehensive set of differential cross sections is measured, including distributions of the jet multiplicities, the jet rapidities, the jet transverse momenta, and the sum of all jet transverse momenta. Furthermore, the Z/γ^* + 2 jet cross section has been measured differentially in a set of variables, related to the dijet system (M_{jj}, ΔR_{jj}, $\Delta\phi_{jj}$, p_T^{jj}). The analysis is based on data corresponding to an integrated luminosity of 8.2 fb^{-1}. Jets are reconstructed using the Run II midpoint algorithm with cone size $R = 0.7$, for $p_T > 30$ GeV and $|y| < 2.1$. The leptons from the Z/γ^* decay are required to have $p_T > 20$ GeV and $|\eta| < 1.0$ and a spatial distance to the nearest jet of $\Delta R > 0.7$. The measurements for the electron and muon channels are performed independently and are combined taking into account asymmetric uncertainties. The data are corrected for detector effects and are compared to predictions from pQCD at NLO (for n = 1,2,3) or LO (n = 4) from BLACKHAT+SHERPA which are corrected for non-perturbative effects. While the p_T and rapidity distributions for Z/γ^* + 1 jet and for Z/γ^* + 2 jet are reasonably well described by theory, theory predicts a significantly lower cross section for Z/γ^* + 3 jet production. The p_T distribution for the third jet is shown in Fig. 5, compared to the theory results in LO and NLO. The large k factor (defined as the ratio of NLO and LO) suggests a poor convergence of the perturbative expansion, and that the failure of NLO could easily be due to missing higher order terms.

4. Event Shapes

Event shape variables have been successfully used in e^+e^- collisions for studying properties of the strong interaction and for determinations of α_s. Recently, resummed theory predictions (NLO+NLL) for event shape variable in hadron-hadron collisions have become available [34]. The CDF collaboration has published measurements of the variables thrust and thrust minor in a data set corresponding to 0.385 fb^{-1} [35]. Jets are defined by an iterative cone jet algorithm (without midpoints). The event shape analysis is performed in an inclusive dijet event sample with both leading jets in the central region ($\eta < 0.7$) and with $E_T^{\max} > 200$ GeV. The event shape variables are defined in the transverse plane, over all final state momenta in the full detector acceptance of $|\eta| < 3.5$. Differential distributions of transverse thrust τ and transverse thrust minor $T_{\min}$ are shown in Figs. 6 and 7. The detector-level data (markers) are compared to PYTHIA [20] (with tune A) on particle level ("Tune A Hadron") and with a detector simulation applied ("Tune A + CDF Sim."). The small differ-

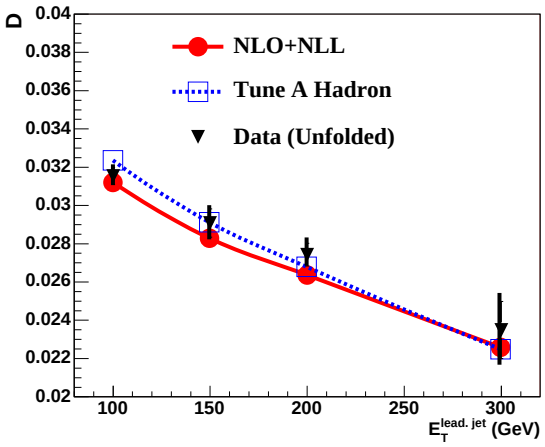

Figure 8: CDF measurement of the "thrust differential" distribution (see text) as a function of the transverse energy of the leading jet.

ence between the two model predictions indicates that detector effects for these event shapes are small. It is seen that while PYTHIA with tune A describes the rough features of the distributions, it does not describe the tails towards small and large values very well. A parton-level theory prediction in NLO+NLL (solid line), computed using NLOJET++ [36, 37] and CAESAR [38, 39], is also overlaid on the data. This calculation does neither include hadronization nor underlying event effects. It was shown in the CDF publication [35] that hadronization corrections are actually small for these variables, but underlying event effects are large. Therefore one can not expect the NLO+NLL calculation to describe the data.

The CDF collaboration has also proposed and measured a new observable, defined as the weighted difference of the mean values of thrust and thrust minor. From analyzing the contributions from hard and soft processes (the latter are assumed to stem from the underlying event) to the mean values of thrust and thrust minor, the authors have identified weighting factors α and β for the averages of both event shapes, such that their weighted difference $(\alpha\langle\tau\rangle - \beta\langle T_{\rm min}\rangle)$ is less sensitive to the soft contributions from the underlying event. An additional correction factor $\gamma_{\rm MC}$ for underlying event contributions was computed using PYTHIA tune A and the variable "thrust differential", D, was then defined as $D = \gamma_{\rm MC}(\alpha\langle\tau\rangle - \beta\langle T_{\rm min}\rangle)$. This variable D was measured as a function of $E_T^{\rm max}$, the leading jet transverse energy in the event. The results, corrected to particle level, are displayed in Fig. 8 (markers) and compared to the particle level prediction from PYTHIA tune A (dotted line) and to the perturbative (parton-level) prediction computed in NLO+NLL (solid line). Both predictions give a good description of the data within the theoretical uncertainties of 20%.

5. Multijet Production

In Run II of the Tevatron, a large number of fundamental jet observables has been measured so far. The inclusive jet cross section has been measured by the CDF and the DØ experiments [40, 41, 42], both using the Run II cone jet algorithm with cone size $R = 0.7$, while CDF has also presented results for the k_T algorithm [43] for a distance parameter of $R = 0.7$, but also for 0.5 and 1.0. The results are presented as double differential cross sections in jet transverse momentum p_T and rapidity y up to $p_T > 500$ GeV. The dijet cross section has been measured by CDF and DØ as a function of dijet invariant mass [44, 45] (the DØ result was also measured as a function of dijet rapidity $|y_{\rm max}|$). Dijet angular distributions have been measured by the DØ experiment in the angular variable $\chi_{\rm dijet} = \exp(|y_1 - y_2|)$ and in different regions of dijet invariant mass, up to above 1 TeV [46].

The analysis of the measured dijet angular distributions has shown no indications for new physics processes which would modify the angular distributions of jets at high dijet invariant masses, such as quark compositeness and extra spatial dimensions. This analysis has produced the best pre-LHC limits on quark compositeness, ADD Large Extra Dimensions, and TeV^{-1} Extra Dimension models. Furthermore, the dijet mass spectra show no evidence for resonances, produced by new heavy particles, decaying into jets. The CDF collaboration has therefore used the dijet mass spectrum to set stringent limits on hypothetical particles such as excited quarks, axigluons, flavor-universal colorons, E6 diquarks, color-octet technirhos, or W' and Z' bosons. Being confident that no new physics processes contribute to the measured jets, the inclusive jet data from both experiments have been used in global PDF analyses [6, 7, 8] exploiting the unique sensitivity of the jet data to the gluon density in the proton at high values of the proton momentum fraction x. Later, however, it has been seen that the rapidity dependence of the DØ dijet data is not well described by all PDFs which were obtained from PDF analyses including the inclusive jet data [45].

Based on the existing studies, one can conclude that inclusive jet and dijet production processes are well understood and modeled adequately in pQCD. It is therefore attractive to extend the QCD jet studies towards larger jet multiplicities probing higher orders in pQCD. Early in Run II, the DØ collaboration has measured dijet

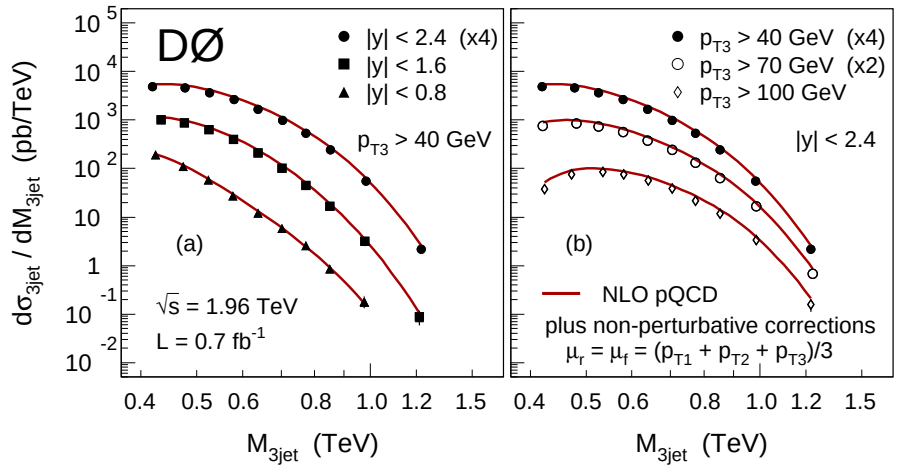

Figure 9: DØ measurement of the three-jet cross section as a function of the three-jet invariant mass in different rapidity regions (left), and for different p_{T3} requirements (right).

azimuthal decorrelations [47], which was a first tests of pQCD predictions using the three-jet matrix elements which have been computed to NLO [36, 37]. Recent measurements extend these studies to different three-jet observables. The DØ collaboration has published a measurement of the three-jet cross section [48], multi-differentially in the three-jet invariant mass, M_{3j}, in the rapidity region for the three jets, and in the p_T requirement for the third jet p_{T3}. A preliminary DØ result measures the ratio of three-jet and dijet cross sections as a function of the leading jet p_T and for different $p_T^{\min}$ requirements for the other jets.

5.1. Three-Jet Cross Section

Jet are defined by the Run II midpoint cone algorithm with cone size $R = 0.7$. The rapidities of the three leading p_T jets are restricted to $|y| < 0.8$, $|y| < 1.6$, or $|y| < 2.4$, alternatively. The p_T requirements are $p_{T1} > 150\,\text{GeV}$ and $p_{T3} > 40\,\text{GeV}$ (with no further requirement for p_{T2}). Additional measurements are made for $p_{T3} > 70\,\text{GeV}$ and $p_{T3} > 100\,\text{GeV}$ (both for $|y| < 2.4$). In all cases, all pairs of the three leading p_T jets are required to be separated by $\Delta R = \sqrt{(\Delta y)^2 + (\Delta\phi)^2} > 2 \cdot R_{\text{cone}} = 1.4$. This separation requirement reduces the phase space in which pairs of the three leading p_T jets are subject to the overlap treatment in the cone jet algorithm. Since this overlap treatment can strongly depend on details of the energy distributions in the overlap area, this region of phase space may not be well modeled by pQCD calculations at lower orders. In the remaining analysis phase space, NLO pQCD calculations are not affected by the Run II cone algorithm's infrared sensitivity [49].

These results [48], displayed in Fig. 9, show the three-jet cross section, differentially in M_{3j} for different rapidity requirements (left) and for different p_{T3} requirements (right). The data are compared to theory predictions which combine NLO pQCD results (computed using FASTNLO [50], based on NLOJET++ [36, 37]) and non-perturbative corrections (computed using PYTHIA with tune DW [51]). The comparison is made for MSTW2008NLO PDFs [52] and the corresponding value of $\alpha_s(M_Z) = 0.120$. The renormalization and factorization scales are set to the average p_T of the three leading p_T jets $\mu_R = \mu_F = \mu_0 = (p_{T1} + p_{T2} + p_{T3})/3$. Ratios of data and theory are shown in Fig. 10 for different PDFs. For MSTW2008NLO PDFs, the ratios of data and theory are almost constant, with only a small dependence on M_{3j} and the $|y|$ and p_{T3} requirements. The central data values are below the central theory predictions by approximately (4–15)% in the different scenarios, slightly increasing with $|y|$ and with p_{T3}. In all cases, the data lie inside the range covered by the renormalization and factorization scale uncertainties (not shown here). Theory for CT10 PDFs [7] (and the corresponding value of $\alpha_s(M_Z) = 0.118$) predicts a different shape for the M_{3j} dependence of the cross section. For $M_{3j} < 0.6\,\text{TeV}$, the results for CT10 PDFs agree with those for MSTW2008NLO, while the CT10 predictions at $M_{3j} = 1.2\,\text{TeV}$ are up to 30% higher. Further theory results are compared to the data for other PDFs, including NNPDFv2.1 [8] ($\alpha_s(M_Z) = 0.119$), ABKM09NLO [53] ($\alpha_s(M_Z) =$

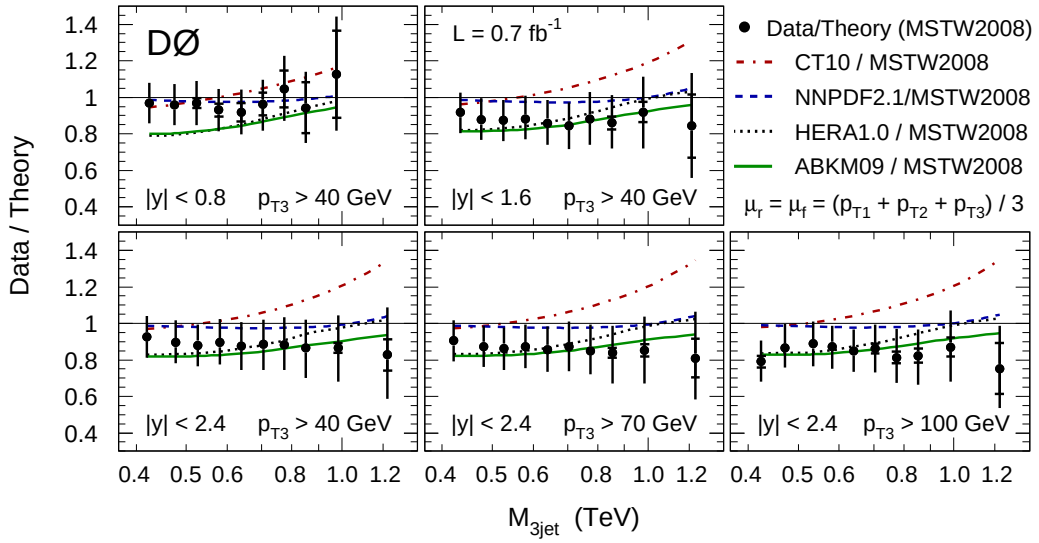

Figure 10: Ratios of data and theory for the DØ three-jet cross section measurement. The ratios are computed for different PDFs and are shown as a function of the three-jet invariant mass in different rapidity regions and for different p_{T3} requirements.

0.1179), and HERAPDFv1.0 [54] ($\alpha_s(M_Z) = 0.1176$). The results for NNPDFv2.1 agree everywhere within ±4% with those from MSTW2008NLO. The cross sections predicted for HERAPDFv1.0 are (15–20)% below those for CT10 everywhere and their M_{3j} distributions have a similar shape. The M_{3j} dependence of the calculations for the ABKM09NLO PDFs is between the shapes of MSTW2008NLO/NNPDFv2.1 and CT10/HERAPDFv1.0. At low M_{3j}, the predictions for ABKM09NLO agree with those for HERAPDFv1.0, while at higher M_{3j}, they predict the smallest cross sections of all PDFs under study.

To quantify the agreement between data and theory, a χ^2 is computed, fully taking into account the correlations of uncertainties [48]. The χ^2 is computed for different scales (for the nominal scale and for variations by factors of 0.5 and 2), for different PDF parametrization, and for different values of $\alpha_s(M_Z)$ used in the NLO matrix elements and PDFs (for all $\alpha_s(M_Z)$ values for which PDF sets are available). The χ^2 results are shown in Fig. 11. For $\alpha_s(M_Z)$ values close to the world average of 0.1184 ± 0.0007 [55], for all PDF sets, with the exception of HERAPDFv1.0, the lowest χ^2 is obtained for the central choice of the scales. From all PDFs, the largest χ^2 values are obtained for CT10 and HERAPDFv1.0 PDFs, independent of the scale and $\alpha_s(M_Z)$ choices. The best overall agreement, corresponding to the lowest χ^2 values, is obtained for MSTW2008NLO for the central scale choice and $\alpha_s(M_Z) = 0.121$, and the results for NNPDFv2.1 are very close.

5.2. Ratio of Three-Jet and Dijet Cross Sections

As discussed above, the interpretation of the three-jet cross section (and any other jet cross section) depends strongly on the choices of $\alpha_s(M_Z)$ and the PDFs. The impact of the latter can be strongly reduced, by studying observables defined as ratios of multijet cross sections. The DØ collaboration has presented a preliminary result [56] for the ratio of the inclusive three-jet and dijet cross sections, $R_{3/2}$, measured as a function of the leading jet transverse momentum $p_T^{\max}$. For this choice, in every $p_T^{\max}$ bin, the numerator is a subset of the denominator, and therefore the variable $R_{3/2}$ represents the conditional probability that a given inclusive dijet event also has a third jet. The value of $p_T^{\max}$ is a common scale for the three-jet and the dijet production processes. Therefore $R_{3/2}(p_T^{\max})$ is directly sensitive to α_s at the scale $\mu_R = p_T^{\max}$ while the PDFs cancel to a large extent in the cross section ratio. In this analysis, the n-jet cross section (for $n = 2, 3$) is defined by all events with n or more jets with p_T above $p_T^{\min}$, in a given rapidity region (here: $|y| < 2.4$ for the n leading jets), for $p_T^{\min} = 50$, 70, 90 GeV. The results are displayed in Fig. 12 as a function of $p_T^{\max}$, for different $p_T^{\min}$ requirements (from left to right). Theory calculations based on NLO pQCD plus non-perturbative corrections are compared to the data for different PDFs (MSTW2008NLO, CT10, NNPDFv2.1, ABKM09NLO) using in all cases $\alpha_s(M_Z) = 0.118$ (in the matrix elements and in the PDFs). In all cases good agreement is seen.

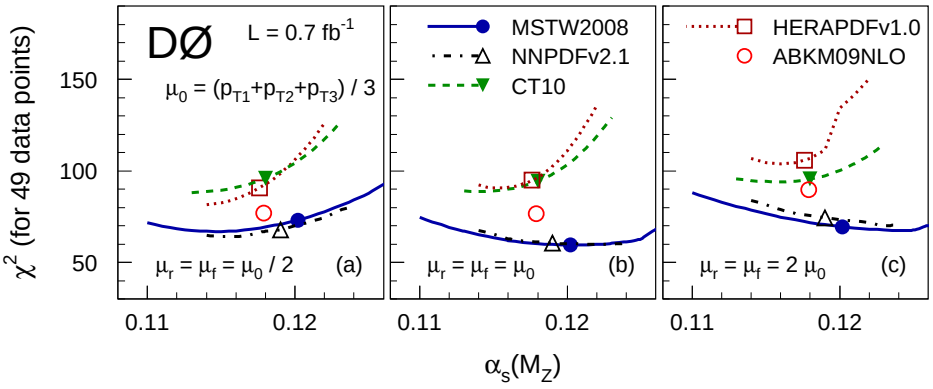

Figure 11: The χ^2 values between data and theory for the three-jet cross section results, displayed as a function of $\alpha_s(M_Z)$ in the theory calculations, for different choices of the scales (from left to right) and for different PDF parametrizations (different lines).

6. Determination of the Strong Coupling Constant

The strong coupling constant, $\alpha_s(M_Z)$, is one of the fundamental parameters of the Standard Model of Particle Physics. The energy dependence of α_s is predicted by the renormalization group equation (RGE). The value of α_s has been determined in many different processes, including a large number of results from hadronic jet production, in either e^+e^- annihilation or in deep-inelastic ep scattering (DIS) up to energies of 209 GeV [55]. Prior to the analysis presented in this article, however, only a single result had been obtained from jet production in hadron-hadron collisions. This result is $\alpha_s(M_Z) = 0.1178^{+0.0081}_{-0.0095}(\text{exp.})^{+0.0071}_{-0.0047}(\text{scale}) \pm 0.0059(\text{PDF})$, extracted by the CDF collaboration from inclusive jet cross section data in $p\bar{p}$ collisions at $\sqrt{s} = 1.8$ TeV [57]. All individual uncertainty contributions for this result are larger than those from comparable results from e^+e^- annihilation or DIS [55].

Recently, the DØ collaboration has presented a new α_s determination [58] with unprecedented precision at a hadron collider. The α_s result is extracted from inclusive jet cross section data in $p\bar{p}$ collisions at $\sqrt{s} = 1.96$ TeV from a recent DØ measurement [41, 42]. The pQCD prediction for the inclusive jet cross section is given by

$$\sigma_{\text{pert}}(\alpha_s) = \left(\sum_n \alpha_s^n c_n\right) \otimes f_1(\alpha_s) \otimes f_2(\alpha_s)\,, \qquad (1)$$

where the c_n are the perturbative coefficients, the $f_{1,2}$ are the PDFs of the initial state hadrons, and the "$\otimes$" sign denotes the convolution over the momentum fractions x_1, x_2 of the hadrons. The sum runs over all powers n of α_s which contribute to the calculation. The DØ result is based on NLO pQCD ($n = 2, 3$) plus 2-loop contributions from threshold corrections [59] ($n = 4$). The latter reduce the scale dependence of the calculations, leading to a significant reduction of the corresponding uncertainties. While the $f_{1,2}$ have no explicit α_s dependence, their knowledge depends on α_s (due to α_s assumptions in the PDF analyses). Since the RGE uniquely relates the value of $\alpha_s(\mu_R)$ at any scale μ_R to the value of $\alpha_s(M_Z)$, all equations can be expressed in terms of $\alpha_s(M_Z)$. The total theory prediction for inclusive jet production is given by the pQCD result in (1), multiplied by a correction factor for non-perturbative effects

$$\sigma_{\text{theory}}(\alpha_s(M_Z)) = \sigma_{\text{pert}}(\alpha_s(M_Z)) \cdot c_{\text{non-pert}}\,. \qquad (2)$$

The pQCD results are computed in FASTNLO, which is based on NLOJET++ and on the calculations from Ref. [59]. To determine $\alpha_s(M_Z)$, recent PDF results are used and $\alpha_s(M_Z)$ is varied in $\sigma_{\text{pert}}(\alpha_s(M_Z))$ (i.e. simultaneously in the matrix elements and in the PDFs) until $\sigma_{\text{theory}}(\alpha_s(M_Z))$ agrees with the data. There are, however, two conceptual issues when extracting α_s from cross section data.

1. When performing the DGLAP evolution of the PDFs, all PDF analyses are assuming the validity of the RGE which has so far been tested only for energies up to 209 GeV. Since extracting α_s at higher energies means testing (and therefore questioning) the RGE, using these PDFs as input would be inconsistent.
2. DØ jet data have been used in all recent global PDF analyses. The PDF uncertainties are therefore correlated with the experimental uncertainties in those kinematic regions in which the DØ jet data had strong impact on the PDF results. As shown in

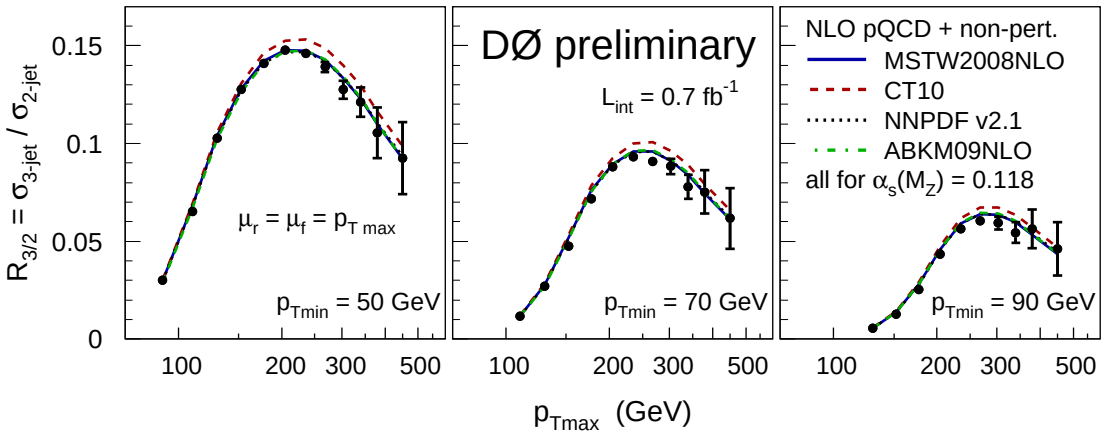

Figure 12: Preliminary DØ results for the ratio of three-jet and dijet cross sections, $R_{3/2}$, as a function of leading jet transverse momentum $p_T^{\max}$ for different $p_T^{\min}$ requirements (from left to right, $p_T^{\min} \geq 50, 70, 90$ GeV). The data are compared to NLO pQCD predictions for different PDFs.

Figs. 51–53 in Ref. [52], this is the case for the proton's gluon density at $x > 0.2 - 0.3$. Since the correlations between PDF uncertainties and experimental uncertainties are not documented, the α_s extraction should avoid using those data points which already had significant impact on the PDF results.

In light of the second issue, the DØ α_s extraction uses only data points which are insensitive to $x > 0.2 - 0.3$. Figure 13 shows the cross section contributions as a function of momentum fractions x (here separately for $x_{\max}$ and $x_{\min}$ in an event) for the inclusive jet cross section bins of the DØ measurement. The (p_T, y) bins in the top left above the solid line have only small contributions from momentum fractions $x > 0.2 - 0.3$. Since all of these data points have p_T below 145 GeV, the first issue does not become relevant here. This leaves 22 (out of 110) inclusive jet data points in the range $50 < p_T < 145$ GeV for the α_s analysis.

The α_s extraction uses PDFs from the MSTW2008 analysis [6] which were obtained at NNLO (consistent with the precision of the theory calculation used here). These PDFs have been determined for 21 $\alpha_s(M_Z)$ values between 0.107 and 0.127 [52]. The continuous $\alpha_s(M_Z)$ dependence of the pQCD cross sections is obtained by interpolating the cross section results for the PDF sets for different $\alpha_s(M_Z)$ values. PDF uncertainties are computed using the twenty uncertainty eigenvectors (corresponding to 68% C.L.). The uncertainties in the pQCD calculation due to uncalculated higher-order contributions are estimated from the $\mu_{R,F}$ dependence of the calculations by varying the renormalization and factorization scales in the range $0.5 \leq (\mu_{R,F}/p_T) \leq 2$. In a first step, data points with the same p_T are combined to determine nine values of $\alpha_s(p_T)$ for $50 < p_T < 145$ GeV. These results are shown in Fig. 14 and compared to results obtained in DIS. A combined determination from all 22 data points yields a result of

$$\begin{aligned}\alpha_s(M_Z) \;=\; & 0.1161^{+0.0034}_{-0.0033}\,(\text{exp.}) \\ & {}^{+0.0010}_{-0.0016}\,(\text{non-pert.}) \\ & {}^{+0.0011}_{-0.0012}\,(\text{PDFs}) \\ & {}^{+0.0025}_{-0.0029}\,(\text{scale}).\end{aligned}$$

This is currently the most precise result from a hadron collider, with similar precision as recent results from jet production in DIS, and consistent with the current world average value [55].

7. Summary

The CDF and DØ collaborations have measured a large number of QCD related observables testing many aspects of the standard model predictions. The high integrated luminosity from the Tevatron allows to explore rare processes like vector boson plus jet production for the first time in great detail. While inclusive photon and diphoton measurements are still challenging theory, other results are in general well described by existing theoretical approximations. Precise measurements of jet observables have strong impact in precision phenomenology, as in constraining the proton PDFs, determinations of α_s, and for excluding new physics models.

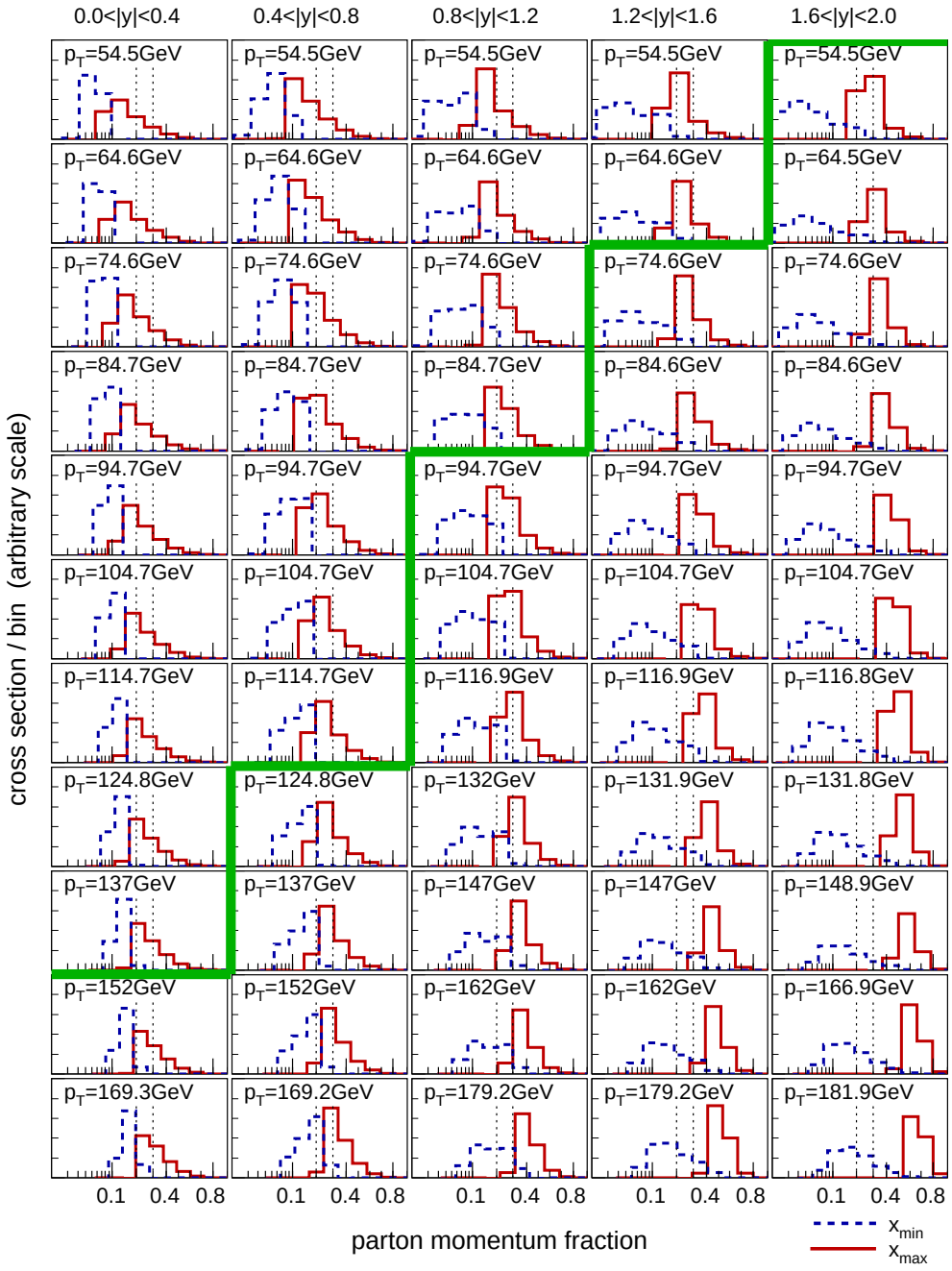

Figure 13: Distributions of the (anti-) proton momentum fractions x_{max} and x_{min} carried by the initial-state partons, for a set of p_T and $|y|$ bins of the inclusive jet cross section, as predicted by NLO pQCD. The (p_T, y) bins which are used in the α_s analysis are the ones to the left (or above) the bold line.

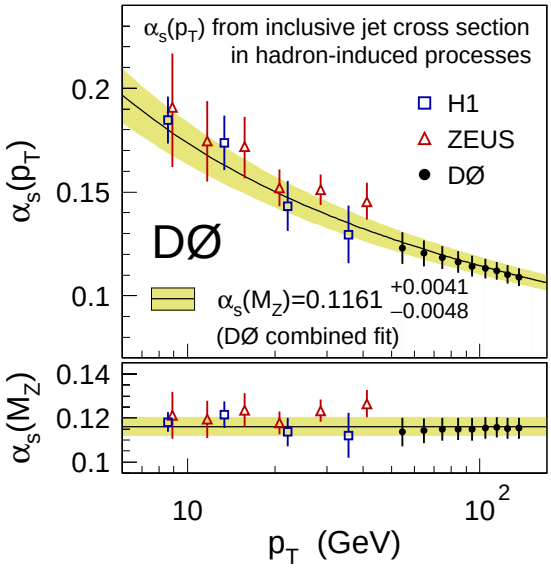

Figure 14: Recent DØ results from a determination of the strong coupling from inclusive jet cross section data, compared to corresponding results in DIS from HERA.

References

[1] C. Buttar *et al.*, in G. Belanger *et al.* (Eds.), *Les Houches 2007, Physics at TeV colliders*, arXiv:0803.0678 [hep-ph], section 9.
[2] H.L. Lai *et al.*, Phys. Rev. D 55, 1280 (1997).
[3] A.D. Martin *et al.*, Eur. Phys. J. C 2, 287 (1998).
[4] P. Aurenche *et al.*, Eur. Phys. J. C 9, 107 (1999).
[5] A.D. Martin *et al.*, Eur. Phys. J. C 4, 463 (1998).
[6] A.D. Martin *et al.*, Eur. Phys. J. C 63, 189 (2009).
[7] H.L. Lai *et al.*, Phys. Rev. D 82, 074024 (2010).
[8] R.D. Ball *et al.*, Nucl. Phys. B 849, 296 (2011).
[9] T. Aaltonen *et al.* [CDF Collaboration], Phys. Rev. D 80, 111106 (2009).
[10] V.M. Abazov *et al.* [D0 Collaboration], Phys. Lett. B 639, 151 (2006) [Erratum-ibid. B 658, 285 (2008)].
[11] T. Binoth, J.P. Guillet, E. Pilon and M. Werlen, Eur. Phys. J. C 16, 311 (2000).
[12] S. Catani, M. Fontannaz, J.P. Guillet and E. Pilon, JHEP 0205, 028 (2002).
[13] J. Pumplin *et al.*, JHEP 0207, 012 (2002).
[14] V.M. Abazov *et al.* [D0 Collaboration], Phys. Lett. B 666, 435 (2008).
[15] V.M. Abazov *et al.* [D0 Collaboration], Phys. Rev. Lett. 102, 192002 (2009).
[16] T. Aaltonen *et al.* [CDF Collaboration], Phys. Rev. D 81, 052006 (2010).
[17] T. Aaltonen *et al.* [CDF Collaboration], Phys. Rev. Lett. 107, 102003 (2011).
[18] V.M. Abazov *et al.* [D0 Collaboration], Phys. Lett. B 690, 108 (2010).
[19] C. Balazs, E.L. Berger, S. Mrenna and C.P. Yuan, Phys. Rev. D 57, 6934 (1998).
[20] T. Sjöstrand *et al.*, Comput. Phys. Commun. 135, 238 (2001).
[21] T. Aaltonen *et al.* [CDF Collaboration], Phys. Rev. D 77, 011108 (2008).
[22] T. Aaltonen *et al.* [CDF - Run II Collaboration], Phys. Rev. Lett. 100, 102001 (2008).
[23] V.M. Abazov *et al.* [D0 Collaboration], Phys. Lett. B 678, 45 (2009).
[24] V.M. Abazov *et al.* [D0 Collaboration], Phys. Lett. B 682, 370 (2010).
[25] T. Aaltonen *et al.* [CDF Collaboration], Phys. Rev. D 79, 052008 (2009).
[26] T. Aaltonen *et al.* [CDF Collaboration], Phys. Rev. Lett. 104, 131801 (2010).
[27] V.M. Abazov *et al.* [D0 Collaboration], Phys. Rev. D 83, 031105 (2011).
[28] V.M. Abazov *et al.* [D0 Collaboration], Phys. Lett. B 666, 23 (2008).
[29] V.M. Abazov *et al.* [D0 Collaboration], Phys. Lett. B 705, 200 (2011).
[30] C.F. Berger *et al.*, arXiv:0905.2735 [hep-ph].
[31] R.K. Ellis *et al.*, JHEP 0901, 012 (2009).
[32] W.T. Giele and G. Zanderighi, JHEP 0806, 038 (2008).
[33] CDF Collaboration, preliminary result (2011). http://www-cdf.fnal.gov/physics/new/qcd/abstracts/zjets_8fb.html
[34] A. Banfi, G.P. Salam and G. Zanderighi, JHEP 0408, 062 (2004).
[35] T. Aaltonen *et al.* [CDF Collaboration], Phys. Rev. D 83, 112007 (2011).
[36] Z. Nagy, Phys. Rev. D 68, 094002 (2003).
[37] Z. Nagy, Phys. Rev. Lett. 88, 122003 (2002).
[38] A. Banfi, G.P. Salam and G. Zanderighi, JHEP 0503, 073 (2005).
[39] A. Banfi, G.P. Salam and G. Zanderighi, Phys. Lett. B 584, 298 (2004).
[40] T. Aaltonen *et al.* [CDF Collaboration], Phys. Rev. D 78, 052006 (2008) [Erratum-ibid. D 79, 119902 (2009)].
[41] V.M. Abazov *et al.* [D0 Collaboration], Phys. Rev. Lett. 101, 062001 (2008).
[42] V.M. Abazov *et al.* [D0 Collaboration], [arXiv:1110.3771 [hep-ex]].
[43] A. Abulencia *et al.* [CDF Collaboration], Phys. Rev. D 75, 092006 (2007) [Erratum-ibid. D 75, 119901 (2007)].
[44] T. Aaltonen *et al.* [CDF Collaboration], Phys. Rev. D 79, 112002 (2009).
[45] V.M. Abazov *et al.* [D0 Collaboration], Phys. Lett. B 693, 531 (2010).
[46] V.M. Abazov *et al.* [D0 Collaboration], Phys. Rev. Lett. 103, 191803 (2009).
[47] V.M. Abazov *et al.* [D0 Collaboration], Phys. Rev. Lett. 94, 221801 (2005).
[48] V.M. Abazov *et al.* [D0 Collaboration], Phys. Lett. B 704, 434 (2011).
[49] G.P. Salam and G. Soyez, JHEP 0705, 086 (2007).
[50] T. Kluge, K. Rabbertz, and M. Wobisch, arXiv:hep-ph/0609285.
[51] M.G. Albrow *et al.*, TeV4LHC QCD Working Group, arXiv:hep-ph/0610012.
[52] A.D. Martin *et al.*, Eur. Phys. J. C 64, 653 (2009).
[53] S. Alekhin *et al.*, Phys. Rev. D 81, 014032 (2010).
[54] F.D. Aaron *et al.* [H1 and ZEUS Collaborations], JHEP 1001, 109 (2010).
[55] S. Bethke, Eur. Phys. J. C 64, 689 (2009), and these proceedings.
[56] V.M. Abazov *et al.* [D0 Collaboration], D0 Conference Note 6032-CONF (2010).
[57] T. Affolder *et al.* [CDF Collaboration], Phys. Rev. Lett. 88, 042001 (2002).
[58] V.M. Abazov *et al.* [D0 Collaboration], Phys. Rev. D 80, 111107 (2009).
[59] N. Kidonakis and J.F. Owens, Phys. Rev. D 63, 054019 (2001).